

PHASES Differential Astrometry and Iodine Cell Radial Velocities of the κ Pegasi Triple Star System

Matthew W. Muterspaugh¹, Benjamin F. Lane¹, Maciej Konacki², Sloane Wiktorowicz²,
Bernard F. Burke¹, M. M. Colavita³, S. R. Kulkarni⁴, M. Shao³

matthew1@mit.edu, blane@mit.edu, maciej@gps.caltech.edu

ABSTRACT

κ Pegasi is a well-known, nearby triple star system. It consists of a “wide” pair with semi-major axis 235 milli-arcseconds, one component of which is a single-line spectroscopic binary (semi-major axis 2.5 milli-arcseconds). Using high-precision differential astrometry and radial velocity observations, the masses for all three components are determined and the relative inclinations between the wide and narrow pairs’ orbits is found to be 43.8 ± 3.0 degrees, just over the threshold for the three body Kozai resonance. The system distance is determined to 34.60 ± 0.21 parsec, and is consistent with trigonometric parallax measurements.

Subject headings: stars:individual(κ Pegasi) – binaries:close – binaries:visual – techniques:interferometric – astrometry – stars:distances

1. Introduction

κ Pegasi (10 Pegasi, ADS 15281, HR 8315, HD 206901; $V \approx 4.1$, $K \approx 3.0$) is comprised of two components, each with F5 subgiant spectrum, separated by 235 milli-arcseconds (here referred to as A and B; for historical reasons, B is the brighter and more massive—this distinction has been the cause of much confusion). Both components A and B have been

¹MIT Kavli Institute for Astrophysics and Space Research, MIT Department of Physics, 70 Vassar Street, Cambridge, MA 02139

²Department of Geological and Planetary Sciences, California Institute of Technology, MS 150-21, Pasadena, CA 91125

³Jet Propulsion Laboratory, California Institute of Technology, 4800 Oak Grove Dr., Pasadena, CA 91109

⁴Division of Physics, Mathematics and Astronomy, 105-24, California Institute of Technology, Pasadena, CA 91125

reported as spectroscopic subsystems (A is in fact only a single star; B is confirmed as a double and the brighter component is designated as Ba, and the unseen companion as Bb). An additional component C is well separated from the other members of the system (13.8 arcseconds) and is faint; this may be optical and is not relevant to the present analysis.

Burnham (1880) discovered the sub-arcsecond A-B binary in 1880. Since this discovery, a number of studies have been carried out to determine the orbit of A-B and to search for additional components. Campbell and Wright (1900) reported a period and semimajor axis for the A-B pair of 11 years and 0.4 arcseconds, respectively, and that the brighter of the stars is a spectroscopic binary with a period “that seems to be about six days.” Luyten (1934) combined all previous observational data to produce a visual orbit between components A and B and a spectroscopic orbit for Ba with period 5.97 days (he interchanged the designations A and B; here his results have been converted to the convention previously mentioned). His work also discredited previous claims that the line of apsides of Ba-Bb varied with the period of the A-B system. Luyten derived a mass for component A of $1.9 M_{\odot}$ and a combined mass for the Ba-Bb subsystem of $3.3 M_{\odot}$. Additionally, because there are no observed eclipses in the Ba-Bb system, he concluded that the maximum possible mass ratio $M_{Ba}:M_{Bb}$ is 3:1. Beardsley and King (1976) obtained separate spectra for components A and B. Their observations confirmed that component B is a 5.97 day single-line spectroscopic binary, and also suggested that A was a spectroscopic binary with period 4.77 days. Barlow and Scarfe (1977) showed that additional observations did not support a subsystem in component A, and suggested that the observations of Beardsley and King suffered from mixed spectra of components A and Ba.

Mayor and Mazeh (1987) have published the most recent spectroscopic orbit for the Ba-Bb subsystem, as well as several measurements of the radial velocity of component A, which also did not confirm the proposed 4.77 day velocity variations. Mayor and Mazeh appear to switch naming conventions for components A and B several times in their paper. They report a mass ratio “ $M_A:M_B = 1.94 \pm 0.6$ ”; this is counter to the tradition of κ Pegasi B being the more massive star, though they later indicate that it is component B that contains the 5.97 day spectroscopic binary. The most recent visual orbit for system A-B was published by Söderhjelm using historical data combined with Hipparcos astrometry (Söderhjelm 1999). Because the period is relatively short and Hipparcos was capable of wide-field astrometry, estimates for the parallax (27.24 ± 0.74 mas), total mass ($4.90 M_{\odot}$), and mass ratio of components A and B ($M_B:M_A = 1.76 \pm 0.11$, in inverse agreement with Mayor & Mazeh) were also possible. Historically, dynamical measurements of the component masses and parallax have been poorly determined for κ Pegasi due to a lack of radial velocity measurements for component A (and Bb), which leave these quantities degenerate.

This paper reports astrometric observations of the A-B system with precisions that allow for detection of the center of light (CL) motion of the Ba-Bb subsystem. These astrometric measurements were obtained as part of the Palomar High-precision Astrometric Search for Exoplanet Systems (PHASES), which aims to detect planets orbiting either component of fifty sub-arcsecond binaries. High-precision iodine-cell radial velocity measurements of κ Pegasi A and Ba obtained with Keck-HIRES are also presented, and a combined double Keplerian, three-dimensional orbital model for the κ Pegasi system is determined. This model allows determination of all three component masses and the distance to the system to within a few percent.

PHASES data are collected at the Palomar Testbed Interferometer (PTI). PTI is located on Palomar Mountain near San Diego, CA (Colavita et al. 1999). It was developed by the Jet Propulsion Laboratory, California Institute of Technology for NASA, as a testbed for interferometric techniques applicable to the Keck Interferometer and other missions such as the Space Interferometry Mission, SIM. It operates in the J ($1.2\mu\text{m}$), H ($1.6\mu\text{m}$), and K ($2.2\mu\text{m}$) bands, and combines starlight from two out of three available 40-cm apertures. The apertures form a triangle with one 110 and two 87 meter baselines.

2. Orbital Models

Basic models have been applied to the astrometric data. The simplifying assumption was made that the Ba-Bb subsystem is unperturbed by star A over the timescale of the observing program, allowing the model to be split into a wide (slow) interaction between star A and the center of mass (CM) of B, and the narrow (fast) interaction between stars Ba and Bb. The results presented in this paper result from modeling both the A-B and Ba-Bb motions with Keplerian orbits.

In general, one cannot simply superimpose the results of the two orbits. The observable in PHASES measurements is the separation of star A and the CL of the Ba-Bb subsystem. Because the CL of Ba-Bb, the CM of Ba-Bb, and the location of star Ba are generally all unequal, a coupling amplitude must be added to the combined model. This coupling amplitude measures the relative size of the semi-major axis of the Ba-Bb subsystem to that of the motion of the CL of the Ba-Bb subsystem. The sign of the superposition is determined by the relative sizes of the mass and luminosity ratios of the stars Ba and Bb. As an example, if the CL is located between the CM of Ba-Bb and the location of star Ba, the motion of the CL will be in opposite direction to the vector pointing from Ba to Bb. For a subsystem

with mass ratio $M_{\text{Bb}}/M_{\text{Ba}}$ and luminosity ratio $L_{\text{Bb}}/L_{\text{Ba}}$, the observed quantity is

$$\vec{y}_{\text{obs}} = \vec{r}_{\text{A-B}} - \frac{M_{\text{Bb}}/M_{\text{Ba}} - L_{\text{Bb}}/L_{\text{Ba}}}{(1 + M_{\text{Bb}}/M_{\text{Ba}})(1 + L_{\text{Bb}}/L_{\text{Ba}})} \vec{r}_{\text{Ba-Bb}} \quad (1)$$

where $\vec{r}_{\text{A-B}}$ is the model separation pointing from star A to the CM of B, and $\vec{r}_{\text{Ba-Bb}}$ is the model separation pointing from star Ba to star Bb. Including this coupling term for astrometric data is important when a full analysis including radial velocity data is made. The light-time effect (LTE) for the finite speed of light across the A-B orbit is included in computing the model of the Ba-Bb orbit.

Alternatively, one can directly combine a model of the A-B system with a model of the motion of the CL of Ba-Bb. For purely astrometric data such a model is appropriate. In this case, there is no sign change for the Ba-Bb CL model, and no extra coupling amplitude is required. This model is used to fit purely astrometric data sets.

$$\vec{y}_{\text{obs}} = \vec{r}_{\text{A-B}} + \vec{r}_{\text{Ba-Bb,C.O.L.}} \quad (2)$$

3. Observations and Data Processing

3.1. PHASES Observations

κ Pegasi was observed with PTI on 52 nights in 2002-2004 using the observing mode described in Lane and Muterspaugh (2004). This method for phase-referenced differential astrometry of subarcsecond binaries is briefly reviewed here.

In an optical interferometer light is collected at two or more apertures and brought to a central location where the beams are combined and a fringe pattern produced. For a broadband source of central wavelength λ the fringe pattern is limited in extent and appears only when the optical paths through the arms of the interferometer are equalized to within a coherence length ($\Lambda = \lambda^2/\Delta\lambda$). For a two-aperture interferometer, neglecting dispersion, the intensity measured at one of the combined beams is given by

$$I(x) = I_0 \left(1 + V \frac{\sin(\pi x/\Lambda)}{\pi x/\Lambda} \sin(2\pi x/\lambda) \right) \quad (3)$$

where x is the differential amount of path between arms of the interferometer, V is the fringe contrast or “visibility”, which can be related to the morphology of the source, and $\Delta\lambda$ is the optical bandwidth of the interferometer assuming a flat optical bandpass (for PTI $\Delta\lambda = 0.4\mu\text{m}$).

The location of the resulting interference fringes are related to the position of the target star and the observing geometry via

$$d = \vec{B} \cdot \vec{S} + \delta_a(\vec{S}, t) + c \quad (4)$$

where d is the optical path-length one must introduce between the two arms of the interferometer to find fringes. This quantity is often called the “delay.” \vec{B} is the baseline, the vector connecting the two apertures. \vec{S} is the unit vector in the source direction, and c is a constant additional scalar delay introduced by the instrument. The term $\delta_a(\vec{S}, t)$ is related to the differential amount of path introduced by the atmosphere over each telescope due to variations in refractive index. For a 100-m baseline interferometer an astrometric precision of $10 \mu\text{as}$ corresponds to knowing d to 5 nm, a difficult but not impossible proposition for all terms except that related to the atmospheric delay. Atmospheric turbulence, which changes over distances of tens of centimeters, angles on order tens of arcseconds, and on subsecond timescales, forces one to use very short exposures (to maintain fringe contrast) and hence limits the sensitivity of the instrument. It also severely limits the astrometric accuracy of a simple interferometer, at least over large sky-angles.

However, in narrow-angle astrometry one is concerned with a close pair of stars, and the observable is a differential astrometric measurement, i.e. one is interested in knowing the angle between the two stars ($\vec{\Delta}_s = \vec{s}_2 - \vec{s}_1$). The atmospheric turbulence is correlated over small angles. If the measurements of the two stars are simultaneous, or nearly so, the atmospheric term subtracts out. Hence it is still possible to obtain high precision “narrow-angle” astrometry.

To correct for time-dependent fluctuations in the atmospheric turbulence, observations consisted of operating PTI in a phase-referenced observing mode. After movable mirrors in the beam-combining lab apply delay compensation to the light collected from two 40 cm apertures, the light from each aperture is split using 30/70 beamsplitters. Seventy percent of the light is sent to the phase-tracking “primary” interferometric beam combiner which measures the time-dependent phase of one star’s interferogram (fringes) caused by the atmospheric turbulence, and used in a feed-back loop to control the optical delay lines.

The other 30% of the light is diverted to the “secondary” interferometric beam combiner. In this system there is an additional delay line with a travel of only ≈ 500 microns. This is used to introduce delay with a sawtooth waveform with frequency on order a Hertz. This allows us to sample the interferograms of all stars in the one arcsecond detector field whose projected separations are within the scan range. Laser metrology is used along all starlight paths between the 30/70 split and the point of interferometric combination to monitor internal vibrations differential to the phase-referencing and scanning beam combiners. For κ

Pegasi, the typical scanning rate in 2002-2003 was one scan per second and four intensity measurements per ten milliseconds; these values were doubled in 2004. The typical scan amplitude was 100 microns. An average of 2189 scans were collected each night the star was observed.

3.2. PHASES Data Reduction

The quoted formal uncertainties in the PHASES data are derived using the standard PHASES data reduction algorithm, which is reviewed here. First, detector calibrations (gain, bias, and background) are applied to the intensity measurements. Next, a grid in differential right ascension and declination is constructed over which to search (in ICRS 2000.0 coordinates). For each point in the search grid the expected differential delay is calculated based on the interferometer location, baseline geometry, and time of observation for each scan. These conversions were simplified using the routines from the Naval Observatory Vector Astrometry Subroutines C Language Version 2.0 (NOVAS-C; see Kaplan et al. (1989)). A model of a double-fringe packet is then calculated and compared to the observed scan to derive a χ^2 value as a merit of goodness-of-fit; this is repeated for each scan, co-adding all of the χ^2 values associated with that point in the search grid. The model fringe template is found by observing single stars, incoherently averaging periodograms of their interferograms, and fitting a sum of Gaussians to the average periodogram. This model effective bandpass is Fourier transformed into delay space to create a model interferogram. Sample data sets have been reanalyzed with a variety of model interferograms and the resulting astrometric solutions vary by less than one μas ; this is largely due to the differential nature of the measurement. Note that in addition to the differential delay there are several additional parameters to the double fringe packet: fringe contrast and relative intensities as well as mean delay. These are all adjusted to minimize χ^2 on a scan-by-scan basis. The final χ^2 surface as a function of differential right ascension and declination is thus derived. The best-fit astrometric position is found at the minimum χ^2 position, with uncertainties defined by the appropriate χ^2 contour—which depends on the number of degrees of freedom in the problem and the value of the χ^2 -minimum.

One potential complication with fitting a fringe to the data is that there are many local minima spaced at multiples of the operating wavelength. If one were to fit a fringe model to each scan separately and average (or fit an astrometric model to) the resulting delays, one would be severely limited by this fringe ambiguity (for a 110-m baseline interferometer operating at $2.2\mu\text{m}$, the resulting positional ambiguity is ~ 4.1 milli-arcseconds). However, by using the χ^2 -surface approach, and co-adding the probabilities associated with all possible

delays for each scan, the ambiguity disappears. This is due to two things, the first being that co-adding simply improves the signal-to-noise ratio. Second, since the observations usually last for an hour or even longer, the associated baseline change due to Earth rotation also has the effect of “smearing” out all but the true global minimum. The final χ^2 -surface does have dips separated by ~ 4.1 milli-arcseconds from the true location, but any data sets for which these show up at the 4σ level are rejected. The final astrometry measurement and related uncertainties are derived by fitting only the 4σ region of the surface.

The PHASES data reduction algorithm naturally accounts for contributions from photon and read-noise. Unmonitored phase noise shows up by increasing the minimum value of χ^2 surface. Comparison of this value with that expected from the number of degrees of freedom allows us to co-add the phase noise to the fit.

This method has been rigorously tested on both synthetic and real data. Data sets are divided into equal sized subsets which are analyzed separately. A Kolmogorov-Smirnov test shows the formal uncertainties from the PHASES data reduction pipeline to be consistent with the scatter between subsets. After an astrometric solution has been determined, one can revisit the individual scans and determine best-fit delay separations on a scan-by-scan basis (the fringe ambiguity now being removed). The differential delay residuals show normal (Gaussian) distribution, and Allan variances of delay residuals agree with the performance levels of the formal uncertainties and show the data to be uncorrelated. It is concluded that the PHASES data reduction pipeline produces measurement uncertainties that are consistent on intranight timescales. Additionally, because components A and Ba are nearly identical (and in particular have equal temperatures to within the uncertainties of the best measurements), potential systematics such as differential dispersion are negligible.

The PHASES measurements have excess scatter about a fit to the double Keplerian model given by eq. 2. Either a scaling factor of 6.637 or a noise floor at $142 \mu\text{as}$ is required to produce a χ_r^2 of unity for the PHASES-only orbit; these values are much larger than observed in other PHASES targets. Because the PHASES analysis has been shown to be consistent on intranight timescales, it is concluded that this excess scatter must occur on timescales longer than a day. Model fit residuals of the PHASES measurements do not show periodic signals, implying the excess scatter is not the result of an additional system component.

Two effects might explain the excess scatter in the PHASES measurements. First, significant variability of either component Ba or Bb would alter the CL position. Hipparcos photometry shows total system photometric scatter only at the level of 4 milli-magnitudes (van Leeuwen et al. 1997); in the extreme case that this scatter were entirely due to variability of component Bb, the astrometric signal would only be of order $35 \mu\text{as}$. The Hipparcos range

in photometric variability is 20 milli-magnitudes; variability on this scale would produce astrometric shifts of scale larger than the observed noise floor, but would require Bb to be an extremely variable star.

A second explanation for the excess scatter may be that the model (equation 1) is not quite the proper model for PHASES observations of triple star systems. In particular, the location of the phase-zero for the Ba-Bb subsystem is not exactly that of its CL; due to the interferometer’s fringe response function, the coupling factor is non-linear and approaches the CL approximation for small separations. If the companion were faint (in this case, a white dwarf), this effect would be negligible and the phase-zero would just be the location of component Ba. If this effect is significant in the κ Pegasi system one might expect to see large amounts of night-to-night scatter in the interferometric visibility ratios between the A and B fringe packets. Unfortunately, the interferograms are much too noisy to allow detection of what is expected to be less than a 4% effect (at the level of the interferogram signal to noise, no scatter is observed in the PHASES interferograms). In comparison to recent PHASES work on the V819 Herculis triple system (Muterspaugh et al. 2005), this effect is more significant for κ Pegasi because the baseline-projected Ba-Bb subsystem separation is sometimes of order the interferometer resolution (the V819 Herculis Ba-Bb subsystem semimajor axis is much smaller and the CL approximation is more appropriate).

For these reasons, PHASES observations are likely better suited to studying planets in binary systems than they are for studying triple star systems. The proposed processes would introduce a noise-floor to the astrometric measurements rather than a scaling to be applied to all uncertainty estimates. Orbital solutions for the triple system were twice computed; once with all PHASES uncertainties increased by a 6.637 scale factor, and again by imposing a 142 μas noise-floor on the PHASES uncertainties. Differences in the fit parameter values represent the systematic errors.

The PHASES differential astrometry measurements are listed in Table 1, in the ICRS 2000.0 reference frame.

Table 1. PHASES data for κ Pegasi

JD-2400000.5	Reweighted Uncertainties								Uncertainties with Noise Floor					N
	δ RA (mas)	δ Dec (mas)	σ_{\min} (μ as)	σ_{maj} (μ as)	ϕ_e (deg)	σ_{RA} (μ as)	σ_{Dec} (μ as)	$\frac{\sigma_{\text{RA,Dec}}^2}{\sigma_{\text{RA}}\sigma_{\text{Dec}}}$	σ_{\min} (μ as)	σ_{maj} (μ as)	σ_{RA} (μ as)	σ_{Dec} (μ as)	$\frac{\sigma_{\text{RA,Dec}}^2}{\sigma_{\text{RA}}\sigma_{\text{Dec}}}$	
52591.15558	139.4192	-68.9527	148.5	2245.9	174.63	2236.1	256.9	-0.81429	142.0	338.4	337.2	144.9	-0.17988	149
52809.42172	176.3305	-52.8124	57.5	2373.4	148.20	2017.3	1251.8	-0.99854	142.0	357.6	313.0	223.8	-0.68878	835
52834.42590	178.7642	-49.5003	55.3	253.1	158.25	235.9	106.9	-0.83218	142.0	142.0	142.0	142.0	0.00000	1756
52836.47700	178.2380	-48.6352	89.0	2518.7	173.84	2504.2	284.3	-0.94917	142.0	379.5	377.6	146.9	-0.23806	736
52862.26351	179.1262	-46.6494	34.6	327.7	144.93	268.9	190.4	-0.97524	142.0	142.0	142.0	142.0	0.00000	3015
52864.43495	180.0359	-45.8604	32.5	635.5	1.42	635.3	36.1	0.43473	142.0	142.0	142.0	142.0	0.00000	1536
52865.25769	180.3088	-45.0103	49.6	770.9	146.66	644.6	425.7	-0.99026	142.0	142.0	142.0	142.0	0.00000	2067
52868.42699	179.3844	-45.8741	23.3	591.6	2.24	591.1	32.9	0.70385	142.0	142.0	142.0	142.0	0.00000	2573
52891.30945	180.2407	-42.5429	33.5	123.8	172.30	122.8	37.1	-0.41400	142.0	142.0	142.0	142.0	0.00000	1935
52893.35153	180.8695	-42.7435	59.7	2076.2	0.77	2076.0	65.9	0.42147	142.0	312.8	312.8	142.0	0.02340	939
52894.33761	181.2314	-42.0489	28.4	251.0	0.66	251.0	28.5	0.10017	142.0	142.0	142.0	142.0	0.00000	2171
52895.31028	181.5086	-41.4518	38.7	142.8	173.23	141.9	42.0	-0.37137	142.0	142.0	142.0	142.0	0.00000	1568
52896.29061	180.7701	-41.3602	22.1	76.5	172.05	75.9	24.3	-0.39859	142.0	142.0	142.0	142.0	0.00000	3320
52897.28730	180.3950	-41.7411	19.0	64.2	171.46	63.6	21.1	-0.41211	142.0	142.0	142.0	142.0	0.00000	4804
52915.28300	180.4724	-39.4518	37.7	173.3	179.51	173.3	37.7	-0.03707	142.0	142.0	142.0	142.0	0.00000	1315
52916.29333	179.8880	-39.7969	53.6	2184.6	1.79	2183.5	86.6	0.78553	142.0	329.1	329.0	142.3	0.05867	1054
52918.11818	181.2814	-38.7883	63.9	3766.3	147.06	3161.0	2048.7	-0.99931	142.0	567.5	482.5	330.8	-0.86317	765
52919.28864	181.3653	-38.3103	24.1	606.1	2.52	605.5	35.9	0.74130	142.0	142.0	142.0	142.0	0.00000	2859
52920.12057	180.8864	-38.2854	73.2	5122.7	148.32	4359.7	2690.8	-0.99949	142.0	771.8	661.1	422.9	-0.91997	936
52929.26987	181.2990	-38.0007	64.8	1315.4	4.54	1311.3	122.6	0.84768	142.0	198.2	197.9	142.4	0.05353	707
52930.25991	181.2730	-37.3111	79.1	1909.0	2.95	1906.5	126.2	0.77828	142.0	287.6	287.3	142.6	0.07860	855
52950.22128	179.7824	-34.3888	94.5	5611.8	7.01	5569.9	691.3	0.99046	142.0	845.5	839.4	174.7	0.57398	480
52952.20159	180.7612	-35.0063	93.8	3396.8	3.52	3390.4	228.7	0.91180	142.0	511.8	510.9	145.2	0.19992	562
52983.12402	179.3421	-30.6844	76.3	2358.2	5.09	2348.9	222.6	0.93893	142.0	355.3	354.1	144.9	0.18272	452
53130.50643	168.6227	-9.8442	85.7	3811.2	143.14	3049.9	2287.0	-0.99890	142.0	574.2	467.3	362.7	-0.87665	1027
53145.46573	168.9574	-7.4882	200.1	14641.9	143.10	11708.9	8793.5	-0.99960	142.0	2206.1	1766.2	1329.6	-0.99106	312
53152.47072	166.1418	-4.9533	48.1	896.3	146.79	750.4	492.5	-0.99317	142.0	142.0	142.0	142.0	0.00000	2389
53168.42321	164.7537	-3.8669	94.4	4229.5	145.84	3500.2	2376.3	-0.99885	142.0	637.3	533.3	376.6	-0.89277	709
53172.46749	162.4907	-2.9062	18.6	183.2	155.52	166.9	77.8	-0.96483	142.0	142.0	142.0	142.0	0.00000	3600
53173.44399	162.7425	-3.3484	28.4	717.8	21.10	669.7	259.8	0.99313	142.0	142.0	142.0	142.0	0.00000	2831
53181.41157	162.9387	-0.9785	29.3	371.5	150.66	324.1	183.8	-0.98317	142.0	142.0	142.0	142.0	0.00000	2322
53182.40964	162.5248	-0.6694	36.5	484.6	150.82	423.5	238.4	-0.98456	142.0	142.0	142.0	142.0	0.00000	2407
53186.41943	161.7325	-0.6729	45.5	590.6	153.56	529.2	266.1	-0.98165	142.0	142.0	142.0	142.0	0.00000	835

3.3. Previous Differential Astrometry Measurements

Previously published differential astrometry measurements made with other methods have been collected and is presented in Table 2 (the complete table available in the electronic version). All of these measurements have been tabulated in either the Washington Double Star Catalog (Mason et al. 2001b) or the Fourth Catalog of Interferometric Measurements of Binary Stars (Hartkopf et al. 2004). In two cases discrepancies were found between the uncertainties listed in the Fourth Catalog and the original sources (the 1982.595 and 1982.852 measurements, both from Tokovinin (1983)); in each case the uncertainties listed in the original work were used. Several data points listed without uncertainty estimates in the Fourth Catalog were found to have uncertainty estimates listed in the original works, in which case those values were used. In several cases a copy of the original source paper could not be obtained; these measurements are flagged in Table 2.

A Keplerian model was fit to the data points for which uncertainty estimates were available to determine whether these were systematically too large or too small, and to find outliers. Measurements were marked as outliers if their fit residual was larger than 3σ in either separation or position angle. Because there were only ten visual/micrometer measurements with published uncertainties (including one outlier), these were not treated as a separate group. There were 43 interferometric measurements with published uncertainty estimates (including four outliers). The uncertainty estimates were found to be systematically too small; this factor was larger in position angle than in separation. Upon iteration, it was found that the separation uncertainties for these 48 data points needed to be increase by a factor of 1.137 and the position angle uncertainties by 2.188. A double Keplerian model (as in eq. 2, to allow for the Ba-Bb subsystem) does not improve the fit; the measurements are insensitive to this small signal.

Most of the previous differential astrometry measurements were published without any associated uncertainties. To allow these to be used in combined fits with other data sets, the average uncertainties were determined as follows. The measurements were separated into subgroups by observational method and each set was analyzed individually; the first group included eyepiece and micrometer observations, and the second contained interferometric observations, including speckle, phase-grating, aperture masking, and adaptive optics. Relative weights were applied to individual measurements as the square root of the number of individual measurements averaged for a given data point. The uncertainties were first estimated to have unit weighting of 10 milli-arcseconds in separation and 1 degree in position angle. A Keplerian model was fit to the data, and residuals in separation and position angle treated individually to update the estimates and outliers removed (again at the 3σ level in either separation or position angle). This procedure was iterated until uncertainties were

Table 1—Continued

JD-2400000.5	Reweighted Uncertainties								Uncertainties with Noise Floor					N
	δRA (mas)	δDec (mas)	σ_{\min} (μas)	σ_{maj} (μas)	ϕ_e (deg)	σ_{RA} (μas)	σ_{Dec} (μas)	$\frac{\sigma_{\text{RA,Dec}}^2}{\sigma_{\text{RA}}\sigma_{\text{Dec}}}$	σ_{\min} (μas)	σ_{maj} (μas)	σ_{RA} (μas)	σ_{Dec} (μas)	$\frac{\sigma_{\text{RA,Dec}}^2}{\sigma_{\text{RA}}\sigma_{\text{Dec}}}$	
53187.40125	162.1831	-0.1186	34.9	503.3	154.19	453.4	221.4	-0.98454	142.0	142.0	142.0	142.0	0.00000	3234
53197.36300	159.6357	0.5078	19.7	198.5	149.30	171.0	102.8	-0.97496	142.0	142.0	142.0	142.0	0.00000	4372
53198.39162	160.0532	1.0905	15.8	140.7	156.01	128.7	59.0	-0.95637	142.0	142.0	142.0	142.0	0.00000	5139
53199.40299	160.6171	1.6181	62.2	1178.0	157.43	1088.0	455.8	-0.98902	142.0	177.5	172.7	147.8	-0.15743	1046
53200.41220	159.4821	1.7555	47.0	2927.0	29.73	2541.7	1452.3	0.99931	142.0	441.0	389.4	251.1	0.76793	1414
53207.41109	157.6318	2.4027	48.9	672.3	33.07	564.0	369.1	0.98745	142.0	142.0	142.0	142.0	0.00000	2391
53208.36518	157.5593	2.1577	37.9	1651.8	24.63	1501.6	689.1	0.99817	142.0	248.9	233.8	165.6	0.40866	2253
53215.32511	156.9988	3.2377	20.0	212.8	151.10	186.6	104.4	-0.97573	142.0	142.0	142.0	142.0	0.00000	4811
53221.38836	156.3834	3.9629	21.0	307.1	35.67	249.8	179.9	0.98966	142.0	142.0	142.0	142.0	0.00000	6197
53228.29947	155.6012	5.6284	18.1	113.4	155.62	103.6	49.6	-0.91724	142.0	142.0	142.0	142.0	0.00000	3450
53229.29186	156.0978	6.1869	20.9	150.8	152.91	134.6	71.1	-0.94423	142.0	142.0	142.0	142.0	0.00000	3851
53233.24062	154.8590	5.5446	62.8	5338.3	145.13	4380.1	3052.3	-0.99969	142.0	804.3	664.9	474.4	-0.93213	691
53234.26794	154.9441	6.3985	20.5	138.3	152.94	123.5	65.5	-0.93639	142.0	142.0	142.0	142.0	0.00000	4093
53235.27795	155.2394	7.0247	20.3	156.2	154.23	140.9	70.3	-0.94743	142.0	142.0	142.0	142.0	0.00000	2679
53236.24000	154.6541	7.2600	40.8	282.9	150.03	245.9	145.7	-0.94659	142.0	142.0	142.0	142.0	0.00000	1184
53249.22289	151.8710	8.8380	19.2	282.1	148.88	241.7	146.8	-0.98828	142.0	142.0	142.0	142.0	0.00000	4247
53270.22848	148.9036	11.8975	49.2	1684.3	160.31	1585.9	569.5	-0.99578	142.0	253.8	243.7	158.7	-0.36294	1474
53285.23449	145.3500	13.9405	33.5	532.2	37.54	422.5	325.4	0.99157	142.0	142.0	142.0	142.0	0.00000	3656
53313.10718	142.2377	18.5964	27.6	652.0	159.78	611.9	226.8	-0.99157	142.0	142.0	142.0	142.0	0.00000	3846

Note. — PHASES data for κ Pegasi. All quantities are in the ICRS 2000.0 reference frame. The reweighted uncertainty values presented in this data have all been scaled by a factor of 6.637 over the formal (internal) uncertainties within each given night. Alternatively, a noise floor is introduced to the uncertainties at a value of $142 \mu\text{as}$; both methods of accounting for excess scatter in the data are used in modeling the system to determine systematic uncertainties. Column 6, ϕ_e , is the angle between the major axis of the uncertainty ellipse and the right ascension axis, measured from increasing differential right ascension through increasing differential declination (the position angle of the uncertainty ellipse’s orientation is $90 - \phi_e$). Introducing a noise floor to the data preserves this orientation angle. The last column is the number of scans taken during a given night.

found consistent with the scatter. Again no improvements were seen in fitting to a double Keplerian model. Of the 358 visual data points, 22 were found to be outliers; the remaining were found to have unit weight average uncertainties of 54.8 milli-arcseconds in separation and 8.94 degrees in position angle. Four of the 44 interferometric data points were found to be outliers; the remaining set was found to have unit weight average uncertainties of 3.83 milli-arcseconds and 1.69 degrees.

While these previous differential astrometry measurements were generally made at different observing wavelengths than the PHASES K-band measurements, their precision is low enough that the wavelength dependency of the Ba-Bb CL is negligible.

3.4. Iodine-cell Radial Velocity Data

Twenty radial velocity measurements for component A and thirty for component Ba were obtained with an iodine gas cell reference using the HIRES spectrometer on the Keck telescopes, using the method described in Konacki (2005). The formal uncertainties of these velocity measurements agree relatively well with scatters about simple models. The component A velocity uncertainties need to be increased by a multiplicative factor of 1.073 to fit a simple linear model ($a + bx$, x is time) with goodness of fit $\chi_r^2 = 1$. The component Ba velocities were fit to a single-Keplerian model representing the Ba-Bb orbital motion combined with a quadratic equation for the CM velocity, which accounts for A-B motion. The component Ba velocity uncertainties must be increased by a multiplicative factor of 1.184 to fit with $\chi_r^2 = 1$. These measurements are listed in Table 3; the uncertainties presented have already been increased by these amounts. The average velocity uncertainty for the (spectrally broad lined) component A is 250 m s^{-1} and that for component Ba is 35 m s^{-1} .

The angle of the Keck-HIRES slit mask is held constant relative to angle on the sky for all observations, and the slit is centered on the CL of the three κ Pegasi components A, Ba, and Bb. Orbital motion of the A-B system changes the position of each star relative to the CL of the system and thus within the slit. These alignment changes are observed as an apparently variable system CM velocity; the signs of these variations for component A are opposite that for the Ba-Bb pair. In the combined 3-dimensional fit with other data sets, this effect is modeled with a polynomial system velocity of

$$V_A = V_{0,Keck} + V_{1,Keck}(t - 53198) + V_{2,Keck}(t - 53198)^2 \quad (5)$$

for component A and

$$V_{Ba} = V_{0,Keck} - R_V (V_{1,Keck}(t - 53198) + V_{2,Keck}(t - 53198)^2) \quad (6)$$

Table 2
Previous Astrometry Measurements

Year	ρ (mas)	θ (deg)	Published		Reweighted		N	Group	Outlier	Source	Reference
			σ_ρ (mas)	σ_θ (deg)	σ_ρ (mas)	σ_θ (deg)					
1880.613	0.32	321.0	0.055	8.9	1	3	1	1	Burnham (1880)
1880.627	0.30	313.7	0.055	8.9	1	3	1	1	Burnham (1880)
1880.725	0.23	319.8	0.055	8.9	1	3	1	1	Burnham (1880)
1880.766	0.22	315.2	0.055	8.9	1	3	1	1	Burnham (1880)
1883.025	0.16	296	0.055	8.9	1	3	1	1	Engelmann (1885)
1998.6896	0.270	293.7	0.010	1.2	0.011	2.6	1	2	1	1	Mason et al. (2001a)
1999.693	0.22	289.0	0.010	2.6	0.011	5.7	1	2	1	1	Gili and Bonneau (2001)
1999.8199	0.230	285.5	0.010	1.2	0.011	2.6	1	2	1	1	Mason et al. (2001a)
1999.8852	0.231	285.0	0.003	0.9	0.003	2.0	1	2	1	1	Mason et al. (2001a)
2000.6196	0.175	276.2	0.003	0.9	0.003	2.0	1	2	1	1	Mason et al. (2001a)

Table 2: Previous differential astrometry data for κ Pegasi. In most cases θ has been changed by 180 degrees from the value appearing in the original works. N represents the number of individual measurements averaged by the original authors. Subset groups are assigned as: 1. visual observations with measurement uncertainties estimated by the original authors, 2. interferometric observations with measurement uncertainties estimated by the original authors, 3. visual observations without measurement uncertainties estimated by the original authors, and 4. interferometric observations without measurement uncertainties estimated by the original authors. A zero in the outlier column indicates the measurement is a $3\text{-}\sigma$ outlier in either ρ or θ and has not been used for fitting. A zero in the source column indicates the original paper could not be found, and secondary references (i.e. the WDS catalog) were used instead; a one indicates the original source was available. The complete table is available in the electronic version.

for component Ba, where t is the time of observation (accounting for the light-time effect) in Modified Julian Date (MJD), and 53198 is an arbitrary offset near the average time of all observations. The best fit is found with fixing $R_V = 1$ without letting it vary as a fit parameter, likely because only the (higher precision) Ba measurements are sensitive to this effect (the size of the required correction is found to be smaller than the component A measurement precisions). Illuminating the slit with a multimode fiber may remove this effect.

The observed spectra do show effects from a third set of spectral lines. These are probably from component Bb; that they can be seen at all indicates this component is too bright to be a white dwarf. A three-dimensional cross-correlation is being developed to obtain velocity measurements for all three components simultaneously, which will be included in a future investigation.

3.5. Previous Radial Velocity Data

Previously published radial velocity measurements from Lick Observatory and CORAVEL have also been collected and reproduced in Table 4 (the complete table available in the electronic version). Each set of radial velocity measurements were fit to double Keplerian models. Luyten (1934) determined the uncertainties of the Lick Observatory velocities presented in Henroteau (1918) at 1.66 km s^{-1} ; these values are found to be consistent in the present study. The CORAVEL velocities from Mayor and Mazeh (1987) required reweighting by a multiplicative factor of 2.31 to be consistent with the scatter about the model.

Three velocities for component A were reported in Mayor and Mazeh (1987). These measurements are discrepant with the other measurements, and are not included in the present fit. Because these velocity measurements were made with a one dimensional cross-correlation algorithm, spectral contamination from component Ba may have biased the A velocities. The broad spectral lines of component A may be more sensitive to spectral blending.

4. Orbital Solution

A combined model for the system was determined by fitting all measurements to equation 1. The fit was repeated twice, once using PHASES data with reweighted uncertainties, and again with a $142 \mu\text{as}$ noise floor for the PHASES data. All plots presented in this paper assume the fit solution in which the $142 \mu\text{as}$ noise floor was imposed. The combined fit with

Table 3
Keck-HIRES Radial Velocities

JD-2400000.5	RV A (km s ⁻¹)	σ_A (km s ⁻¹)	RV Ba (km s ⁻¹)	σ_{Ba} (km s ⁻¹)
52961.26742			30.6932	0.0358
52961.30804			29.4782	0.0368
52961.38225			27.0732	0.0377
52962.25385			-8.9328	0.0346
52962.29817			-10.8228	0.0347
52962.37163			-14.0178	0.0378
52962.37825			-14.3178	0.0384
53094.64549			-42.7248	0.0374
53094.64687			-42.7958	0.0369
53094.65230			-42.8538	0.0378
53205.36826	-20.1918	0.2499	39.5022	0.0318
53205.37367	-20.1978	0.2138	39.4852	0.0352
53205.40455	-20.1938	0.2551	39.5292	0.0314
53205.40589	-20.0458	0.2501	39.4652	0.0318
53205.45277	-20.2498	0.2337	39.5232	0.0334
53205.45679	-20.0298	0.2137	39.4502	0.0363
53205.49655	-19.8808	0.2037	39.2702	0.0377
53205.49792	-19.8688	0.2046	39.3172	0.0365
53205.55404	-20.0027	0.3180		
53205.55811	-20.0847	0.3032		
53276.30124	-19.6247	0.2562	25.5523	0.0350
53276.30196	-19.8067	0.2554	25.5453	0.0350
53276.39785	-19.3757	0.2648	28.5373	0.0340
53276.40044	-19.5267	0.3083	28.6253	0.0328
53276.47261	-19.1697	0.2747	30.6663	0.0333
53276.47322	-19.1787	0.2669	30.6823	0.0332
53277.25969	-18.8347	0.2734	38.0633	0.0445
53277.26627	-18.9937	0.2201	37.9723	0.0349
53277.29652	-19.0287	0.2141	37.6463	0.0328
53277.29817	-18.9047	0.2155	37.6093	0.0329
53328.28414			-42.1537	0.0329
53328.33982			-40.8997	0.0336

Table 3: Keck-HIRES iodine-cell radial velocity data of κ Pegasi. The uncertainties presented have been scaled from the formal (internal) uncertainties to reflect the scatter about a best-fit models. The scaling factor for component A velocities was 1.073; for Ba, it was 1.184.

Table 4
Previous Radial Velocity Measurements

JD-2400000.5	RV Ba (km s ⁻¹)	σ_{Ba} (km s ⁻¹)	Set
13803.285	-36.35	1.66	1
15238.322	35.74	1.66	1
15239.317	27.92	1.66	1
15240.328	-11.09	1.66	1
15244.332	37.71	1.66	1
45625.815	-23.75	1.016	2
45627.768	30.05	1.016	2
45676.770	-6.76	1.109	2
46028.882	0.40	1.109	2
46120.213	-55.45	1.063	2

Table 4: Previous Radial Velocity Measurements for κ Pegasi Ba. Set 1 is Lick Observatory data from Henroteau (1918); Luyten (1934) determined the uncertainties of this data set from the scatter to a model at 1.66 km s⁻¹; these values are consistent with the present solution. Set 2 is CORAVEL data from Mayor and Mazeh (1987); the uncertainties have been reweighted by a factor of 2.31 from the original work, in order that they might be combined with other data sets for a simultaneous fit. The complete table is available in the electronic version.

PHASES data uncertainties reweighted has a minimized reduced $\chi_r^2 = 1.161$; for the combined fit with a $142 \mu\text{as}$ PHASES noise floor $\chi_r^2 = 1.165$. The fits have 22 free parameters and 1061 degrees of freedom; the values for χ_r^2 are slightly higher than one would expect, likely resulting from the way in which several of the uncertainties had to be estimated. The uncertainties presented for all fit parameters in Table 5 have been increased by a factor of $\sqrt{\chi_r^2}$. The combined orbital model is plotted in Figures 1 (the A-B orbit) and 2 (the Ba-Bb orbit).

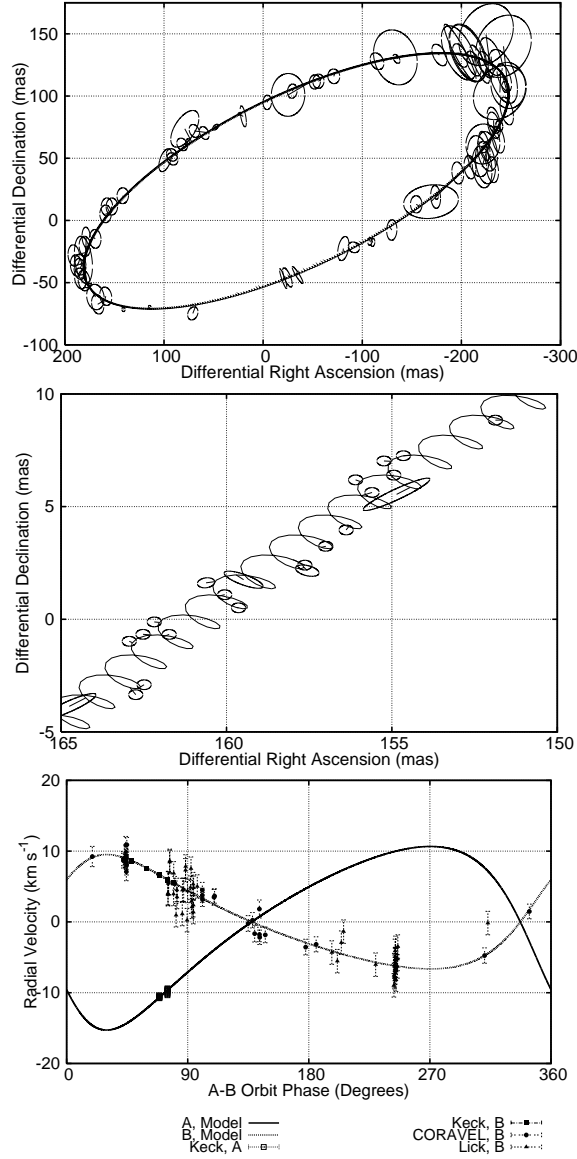


Fig. 1.— The orbit of κ Pegasi A-B. (Top) The complete A-B orbit plotted with the uncertainty ellipses for previous differential astrometry measurements. For clarity, only previous astrometry measurements for which all dimensions of the uncertainty ellipses are smaller than 20 milli-arcseconds are plotted. (Middle) A portion of the PHASES measurements from the 2004 observing season; the CL motion of the Ba-Bb orbit is superimposed on the A-B (wide) orbit. A noise floor of 142 μ as has been imposed on the PHASES measurements as discussed in the text. (Bottom) Component A and Ba radial velocity measurements; the system CM velocities and Ba-Bb motion have been removed from the radial velocity graph. Phase zero is at periastron passage.

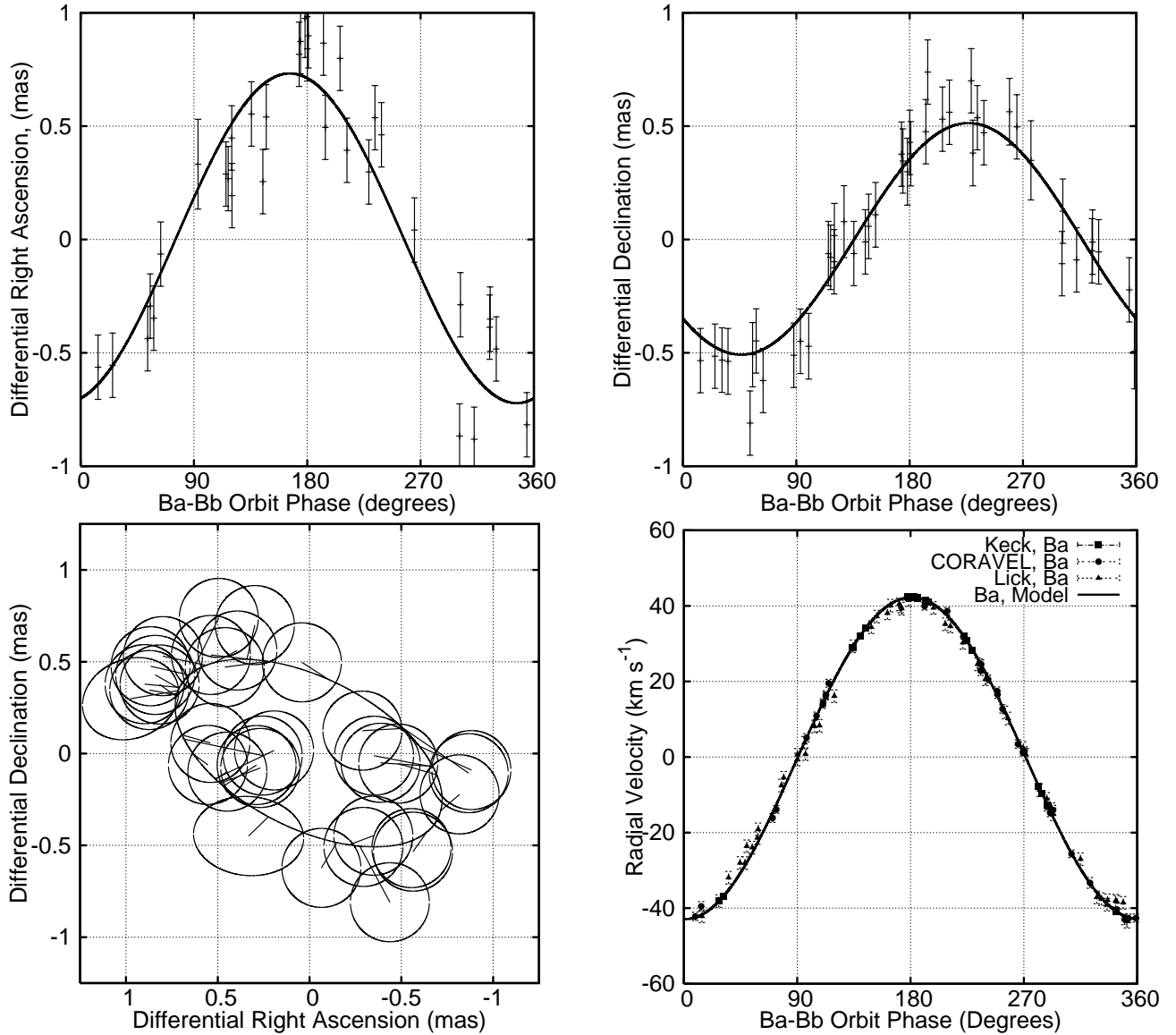


Fig. 2.— The orbit of κ Pegasi Ba-Bb. (Top Left and Right, Bottom Left) Apparent astrometric orbit of the Ba-Bb CL, plotted with PHASES measurements (with the A-B motion removed). A noise floor of $142 \mu\text{as}$ has been imposed on the PHASES measurements as discussed in the text. Only measurements with uncertainties less than $200 \mu\text{as}$ are plotted. (Top) Differential right ascension (Left) and declination (right) versus orbital phase; phase zero is at periastron passage. (Bottom Left) Only those measurements for which all dimensions of the uncertainty ellipses are smaller than $200 \mu\text{as}$ are plotted. (Bottom Right) Radial velocity of component Bb; system CM velocities and A-B orbit velocities have been removed.

Table 5. Orbit models for κ Pegasi

	Martin et al. (1998) Hartkopf et al. (1989)	Söderhjelm (1999)	PHASES Reweight + Pre. + RV	PHASES 142 μ s floor + Pre. + RV	Combined Average and Uncertainties
P_{A-B} (days)	4237 \pm 44*	4233*	4227.11 \pm 0.55	4226.99 \pm 0.55	4227.05 \pm 0.55
$T_{0,A-B}$ (MJD)	43950 \pm 9.9 (52424) [†]	48188 (52422) [†]	52399.3 \pm 1.8	52396.7 \pm 2.0	52398.0 \pm 2.0
e_{A-B}	0.313 \pm 0.009	0.31	0.3177 \pm 0.0014	0.3183 \pm 0.0015	0.3180 \pm 0.0015
i_{A-B} (degrees)	108.04 \pm 0.50	108	107.859 \pm 0.023	107.886 \pm 0.028	107.872 \pm 0.028
ω_{A-B} (degrees)	304.17 \pm 0.60	305	304.25 \pm 0.19	304.03 \pm 0.21	304.14 \pm 0.21
Ω_{A-B} (degrees)	288.85 \pm 0.60	290	109.101 \pm 0.050	109.178 \pm 0.057	109.140 \pm 0.057
P_{Ba-Bb} (days)	5.9714971 \pm 1.3 \times 10 ⁻⁶	5.9714971 \pm 1.3 \times 10 ⁻⁶	5.9714971 \pm 1.3 \times 10 ⁻⁶
$T_{0,Ba-Bb}$ (MJD)	52402.225 \pm 0.097	52402.225 \pm 0.097	52402.225 \pm 0.097
e_{Ba-Bb}	0.0073 \pm 0.0013	0.0073 \pm 0.0013	0.0073 \pm 0.0013
i_{Ba-Bb} (degrees)	128.6 \pm 1.5	121.2 \pm 3.2	124.9 \pm 3.7
ω_{Ba-Bb} (degrees)	359.1 \pm 5.8	359.1 \pm 5.9	359.1 \pm 5.9
Ω_{Ba-Bb} (degrees)	63.99 \pm 0.91	63.0 \pm 2.1	63.5 \pm 2.1
$V_{0,Keck}$ (km s ⁻¹)	-9.51 \pm 0.21	-9.47 \pm 0.21	-9.49 \pm 0.21
$V_{1,Keck}$ (km s ⁻¹ day ⁻¹)	-2.9 \times 10 ⁻⁴ \pm 3.3 \times 10 ⁻⁴	-2.4 \times 10 ⁻⁴ \pm 3.3 \times 10 ⁻⁴	-2.6 \times 10 ⁻⁴ \pm 3.3 \times 10 ⁻⁴
$V_{2,Keck}$ (km s ⁻¹ day ⁻²)	6.8 \times 10 ⁻⁶ \pm 2.3 \times 10 ⁻⁶	6.9 \times 10 ⁻⁶ \pm 2.3 \times 10 ⁻⁶	6.9 \times 10 ⁻⁶ \pm 2.3 \times 10 ⁻⁶
$V_{0,C}$ (km s ⁻¹)	-9.42 \pm 0.25	-9.40 \pm 0.25	-9.41 \pm 0.25
$V_{0,Lick}$ (km s ⁻¹)	-8.26 \pm 0.25	-8.26 \pm 0.25	-8.26 \pm 0.25
M_A (M_\odot)	1.562 \pm 0.197	1.78 \pm 0.16	1.549 \pm 0.049	1.549 \pm 0.050	1.549 \pm 0.050
M_{Ba+Bb} (M_\odot)	2.602 \pm 0.284	3.13 \pm 0.27	2.464 \pm 0.076	2.487 \pm 0.077	2.476 \pm 0.077
M_{Bb}/M_{Ba}	0.524 \pm 0.018	0.456 \pm 0.024	0.490 \pm 0.034
L_{Bb}/L_{Ba}	0.009 \pm 0.013	0.000 \pm 0.020	0.004 \pm 0.020
d (parsecs)	34.55 \pm 0.21	34.66 \pm 0.21	34.60 \pm 0.21
$K_{p,A} - K_{p,B}$ (Magnitudes)	0.190 \pm 0.001
M_{Ba} (M_\odot)	1.662 \pm 0.064
M_{Bb} (M_\odot)	0.814 \pm 0.046
a_{A-B} (AU)	8.139 \pm 0.062
a_{Ba-Bb} (AU)	0.08715 \pm 0.00090
π (mas)	28.63 \pm 0.92	27.24 \pm 0.74	28.90 \pm 0.18

Note. — Orbit models for κ Pegasi. Pre.: Previous differential astrometry measurements, listed in Table 2. Uncertainties in the final column are the maximum of three uncertainties: the uncertainty from the combined fit that included PHASES-reweighted data, that including PHASES data with a 142 μ s noise floor, and the difference in the fit values for the two models. The luminosity ratio L_{Bb}/L_{Ba} is for K-band observations. $K_{p,A} - K_{p,B}$ is derived from Keck adaptive optics imaging rather than from PHASES measurements. The final five parameters are derived from

the other quantities; their uncertainties are determined via error propagation.

* Converted from years in original work.

‡ Converted from years in original work, quantity in parenthesis converts to common epoch.

No evidence supporting additional companions is seen, including the proposed 4.77-day period companion to κ Pegasi A. The suggested amplitude for the velocity curve in Beardsley & King was roughly 30 km s^{-1} , corresponding to astrometric motion of star A on order 1.1 mas, an effect that would be seen in the PHASES astrometric data if present. The data residuals are plotted in Figures 3 and 4.

4.1. Eccentricity and Mutual Inclination

A small—but non-zero—eccentricity is found in the Ba-Bb system. The main sequence age for $1.6 M_{\odot}$ stars is of order 2.5 gigayears (Gyr); the subgiant luminosity classes of components A and Ba implies the system age is likely near this value. Tidal circularization of the Ba-Bb system is predicted to occur on Gyr timescales (Zahn 1977); tidal circularization explains the low eccentricity only if three-body dynamics do not dominate the evolution of the Ba-Bb eccentricity.

The mutual inclination Φ of two orbits is given by

$$\cos \Phi = \cos i_1 \cos i_2 + \sin i_1 \sin i_2 \cos (\Omega_1 - \Omega_2) \quad (7)$$

where i_1 and i_2 are the orbital inclinations and Ω_1 and Ω_2 are the longitudes of the ascending nodes. The combined fit gives a value of 43.8 ± 3.0 degrees for the relative inclinations of the A-B and Ba-Bb orbits. This represents only the sixth system for which unambiguous determination of the mutual inclination is possible.

The mutual inclination of the κ Pegasi system is found to be just over the threshold (39.2 degrees) required for the Kozai Mechanism to drive inclination-eccentricity oscillations in the Ba-Bb system (Kozai 1962). The maximum eccentricity found in such oscillations is given by Innanen et al. (1997) as

$$e_{\max} = \sqrt{1 - (5/3) \cos^2 (\Phi_0)} \quad (8)$$

where Φ_0 is the mutual inclination at small eccentricity states. For a mutual inclination of 43.8 ± 3.0 degrees, e_{\max} is in the range $0.36_{-0.10}^{+0.15}$. While the fit solution shows a slight (1.5σ) preference for a mutual inclination for which Kozai oscillations will occur, the uncertainty is such that a lack of such oscillations would not be a complete surprise. The period of Kozai oscillations would be of order 10^4 years (Kiseleva et al. 1998); this is much shorter than predicted tidal circularization timescales. An insignificant amount of orbital energy would be lost to tidal heating over the course of each oscillation, and the Kozai Mechanism would dominate the evolution of the eccentricity of the Ba-Bb subsystem. Over the life of the system, it is possible that some orbital energy is lost to tidal heating.

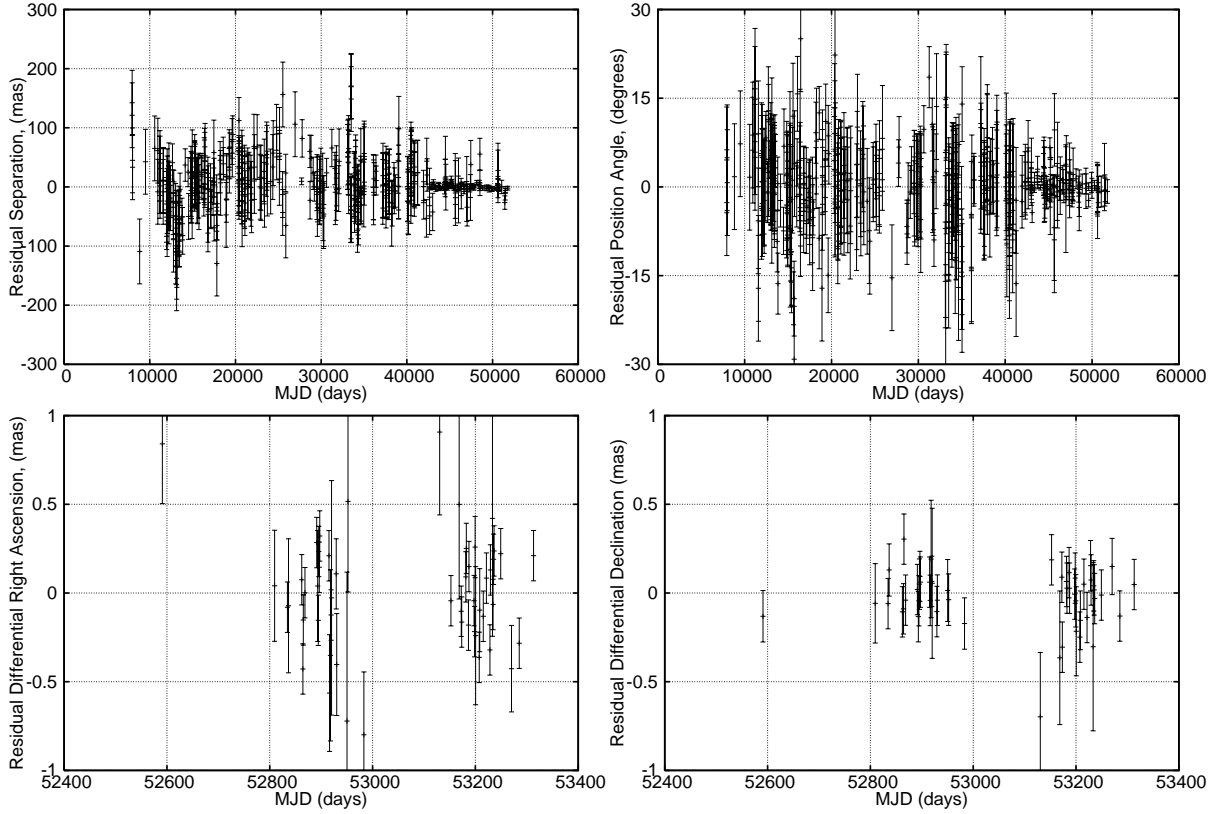


Fig. 3.— Residuals for differential astrometry of κ Pegasi. (Top) Separation (left) and position angle (right) residuals to the combined model for previous astrometric measurements. (Bottom) Right ascension (left) and declination (right) residuals to the combined model for PHASES measurements. A noise floor of $142 \mu\text{as}$ has been imposed on the PHASES measurements as discussed in the text.

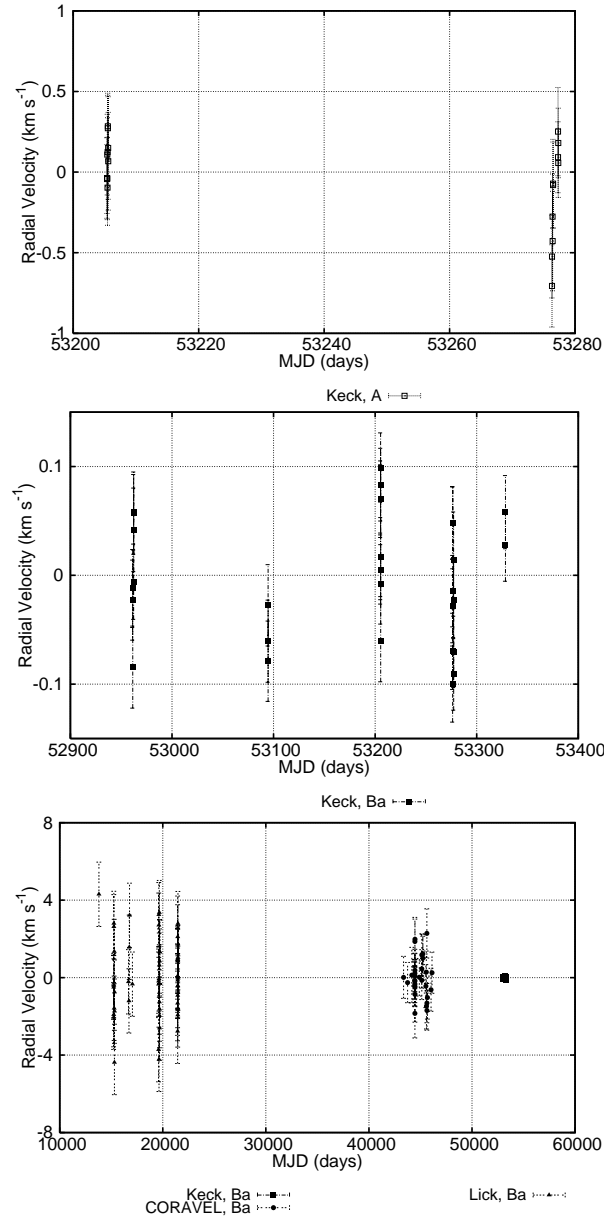


Fig. 4.— Residuals for radial velocimetry of κ Pegasi. (Top) Component A velocity residuals to the combined model. (Middle) Keck-HIRES component Ba velocity residuals to the combined model. (Bottom) All component Ba velocity residuals to the combined model.

The current small value for the Ba-Bb eccentricity tempts one to conclude that Kozai oscillations do not occur (i.e. that the true mutual inclination is on the lower side of the 39.2 degrees threshold), but it is also possible that it is simply being observed at a fortunate time. Over the ninety years over which radial velocity measurements of Ba have been made, one might expect to see variations in the Ba-Bb eccentricity of order a fraction of a percent. The Lick and CORAVEL radial velocity measurements by themselves each only determine the Ba-Bb eccentricity to the level of a percent, thus one cannot measure whether significant Kozai-induced eccentricity variations have occurred.

4.2. Parallax

The combined astrometric and RV model is used to determine the distance to the system, and in turn a value of 28.90 ± 0.18 milli-arcseconds for the system parallax. This value agrees well with the trigonometric parallax determined from Hipparcos astrometry by Martin et al. (1998), who reprocessed the Hipparcos astrometry using the A-B orbital model of Hartkopf et al. (1989) for CL astrometric corrections; their value is 28.63 ± 0.92 . The raw Hipparcos trigonometric parallax of 28.34 ± 0.88 milli-arcseconds also agrees well (Perryman et al. 1997).

The revised Hipparcos analysis of Söderhjelm (1999) gives a value of 27.24 ± 0.74 , which does not agree well with the other results. Also discrepant is the original (ground-based) trigonometric parallax measurement of 35.6 ± 3.2 of van de Kamp (1947). It should be noted that for much of the history of the system’s study, the parallax of van de Kamp was used to estimate the total system mass, leading to discrepant values. Both of these do agree at the 3σ level, and it is concluded that the present value of 28.90 ± 0.18 is most consistent with all observations.

4.3. Component Masses and Stellar Evolution

Components A and Ba are of roughly equal mass (at $M_A = 1.549 \pm 0.050M_\odot$ and $M_{Ba} = 1.662 \pm 0.064$), and were likely late-type A or early F dwarf stars before evolving to their present state slightly off the main sequence. The measured mass for component Bb ($M_{Bb} = 0.814 \pm 0.046M_\odot$) indicates it is likely a late-type G or early K dwarf. The third set of lines are observed in the Keck-HIRES spectra supports identification of this component as a late G/early K dwarf rather than a white dwarf remnant of a much more massive star. At near-infrared K-band, the expected luminosity of a late G/early K dwarf is 7% that of

either component A or Ba; while not in perfect agreement with the combined fit value for the luminosity ratio, this does indicate the low value is appropriate and astrometric effects due to a luminous third component are small.

The κ Pegasi system is valuable to modeling stellar evolution as masses for all three components are well-constrained, and two slightly evolved stars can be assumed coevolved with the faint dwarf component Bb. Differential magnitudes for all system components (which can perhaps be determined from the Keck-HIRES spectra in a later investigation) are required for proper evolutionary modeling.

Keck adaptive optics observations of κ Pegasi on MJD 53227.44 determine a differential magnitude between component A and combined light for Ba and Bb of 0.188 ± 0.001 magnitudes in a narrow band H_2 2-1 filter centered at 2.2622 microns. Observations of similar spectral type 20 Persei (F4V+F6V) during the same evening in both the narrow band filter and astronomical K_p band are used to approximate the K_p band differential magnitude as 0.190 ± 0.001 . Better measurement of the relative intensities of Ba and Bb is required to constrain stellar models.

5. Conclusions

The PHASES measurements provide detection of the κ Pegasi Ba-Bb subsystem CL motion for the first time. This allows the mutual inclinations of the wide and narrow orbits to be determined; this is only the sixth such determination that has been made. The high value for the relative inclination implies the narrow (Ba-Bb) pair may undergo eccentricity-inclination oscillations caused by the Kozai mechanism. No evidence for additional system components is observed.

Combined with radial velocity observations, the distance to the κ Pegasi system is determined to a fifth of a parsec. The distance agrees well with that determined by Hipparcos astrometry, and is of higher precision. Masses for each component are determined at the level of a few percent; continued observations—particularly to determine additional velocities for component A (or the first velocities for Bb)—will improve these mass measurements. Future investigations of this system to determine the relative luminosities of the three components will allow model fitting of the components’ evolutions, of particular interest because two components have evolved slightly off the main sequence.

We thank the support of the PTI collaboration, whose members have contributed designing an extremely reliable instrument for obtaining precision astrometric measurements.

We acknowledge the extraordinary efforts of K. Rykoski, whose work in operating and maintaining PTI is invaluable and goes far beyond the call of duty. Observations with PTI are made possible through the efforts of the PTI Collaboration, which we acknowledge. Part of the work described in this paper was performed at the Jet Propulsion Laboratory under contract with the National Aeronautics and Space Administration. Interferometer data was obtained at the Palomar Observatory using the NASA Palomar Testbed Interferometer, supported by NASA contracts to the Jet Propulsion Laboratory. This research has made use of the Washington Double Star Catalog maintained at the U.S. Naval Observatory. This research has made use of the Simbad database, operated at CDS, Strasbourg, France. MWM acknowledges the support of the Michelson Graduate Fellowship program. BFL acknowledges support from a Pappalardo Fellowship in Physics. MK is supported by NASA through grant NNG04GM62G. PHASES is funded in part by the California Institute of Technology Astronomy Department.

REFERENCES

- R. G. Aitken. Bulletin No. 11 - Observations of 194 double stars. *Lick Observatory Bulletin*, 1:66–81, January 1900a.
- R. G. Aitken. Measures of 204 Double Stars. *Astronomische Nachrichten*, 152:209–+, June 1900b.
- R. G. Aitken. *Publications of Lick Observatory*, 12:1, 1914.
- R. G. Aitken. Bulletin Number 348 - Measures of a selected list of double stars. *Lick Observatory Bulletin*, 11:58–98, 1923.
- R. G. Aitken. Measures of double stars in the years 1923-1926. *Lick Observatory Bulletin*, 12:173–182, 1924.
- R. G. Aitken. Measures of 84 double stars in the years 1927-1935. *Lick Observatory Bulletin*, 17:91–98, 1935.
- E. Aristidi, M. Carillet, J.-L. Priour, B. Lopez, Y. Bresson, and L. Koechlin. ICCD speckle observations of binary stars: Measurements during 1994-1995. *A&AS*, 126:555–561, December 1997.
- M. P. Baize. Mesures d'étoiles doubles faites à l'équatorial de o^m,305 de l'Observatoire de Paris. *Journal des Observateurs*, 28:41–+, January 1945.
- P. Baize. Mesures d'étoiles doubles. *Journal des Observateurs*, 23:95–+, January 1940.

- P. Baize. Mesures d'étoiles doubles faites à l'Observatoire de Paris. *Journal des Observateurs*, 37:73–+, January 1954.
- I. Balega, D. Bonneau, and R. Foy. Speckle interferometric measurements of binary stars. II. *A&AS*, 57:31–36, July 1984.
- I. I. Balega and Y. Y. Balega. Digital speckle interferometry of binary stars with the six-meter telescope. *Soviet Astronomy Letters*, 13:208–+, May 1987.
- I. I. Balega, Y. Y. Balega, I. N. Belkin, A. F. Maximov, V. G. Orlov, E. A. Pluzhnik, Z. U. Shkhagosheva, and V. A. Vasyuk. Binary star speckle measurements during 1989–1993 from the SAO 6 M and 1 M telescopes in Zelenchuk. *A&AS*, 105:503–506, June 1994.
- I. I. Balega, Y. Y. Balega, I. N. Belkin, V. A. Vasyuk, and A. F. Maksimov. Television speckle interferometry of binary stars at the Zeiss-1000 telescope. *Bull. Special Astrophys. Obs.*, 35:9–14, 1993.
- I. I. Balega, Y. Y. Balega, A. F. Maksimov, E. A. Pluzhnik, Z. U. Shkhagosheva, and V. A. Vasyuk. Binary star speckle measurements during 1992–1997 from the SAO 6-m and 1-m telescopes in Zelenchuk. *A&AS*, 140:287–292, December 1999.
- I. I. Balega, Y. Y. Balega, and V. A. Vasyuk. Speckle Interferometry Measurements of Binaries Using the 6-METER Telescope in 1986. *BULL. SPECIAL ASTROF.OBS. NORTH CAUCASUS V. 28, P. 102, 1989*, 28:102–+, 1989.
- Y. Y. Balega and I. I. Balega. Digital Speckle Interferometry of 72 Binary Stars. *Soviet Astronomy Letters*, 11:47–+, February 1985.
- D. J. Barlow and C. D. Scarfe. Kap Peg, a triple system. *PASP*, 89:857–861, December 1977.
- E. E. Barnard. Micrometrical measures of double stars. *AJ*, 19:113–116, October 1898.
- E. E. Barnard. cited by Lewis. *Memoirs of the Royal Astronomical Society*, 56:1, 1906.
- W. R. Beardsley and M. W. King. Interpretation of a spectrographic observations of the resolved components of kap Peg. *PASP*, 88:200–203, April 1976.
- A. L. Behall. *Unpublished*.
- E. Bernewitz. *Publ. Berlin Babelsberg Obs.*, 14 Pt. 1, 1962.

- A. Blazit, D. Bonneau, L. Koechlin, and A. Labeyrie. The digital speckle interferometer : preliminary results on 59 stars and 3C 273. *ApJ*, 214:L79–L84, June 1977.
- D. Bonneau, J. M. Carquillat, and J. L. Vidal. Observations of binary stars by speckle interferometry at the PIC DU Midi T2m. *A&AS*, 58:729–733, December 1984.
- W. M. Bowyer. *Greenwich Observations*, 1898.
- W. M. Bowyer. *Greenwich Observations*, 1899.
- W. M. Bowyer. *Greenwich Observations*, 1900.
- W. M. Bowyer. *Greenwich Observations*, 1901.
- W. M. Bowyer. *Greenwich Observations*, 1903.
- W. M. Bowyer. *Greenwich Observations*, 1904.
- W. M. Bowyer. *Greenwich Observations*, 1905.
- W. M. Bowyer. *Greenwich Observations*, 1906.
- W. M. Bowyer. *Greenwich Observations*, 1907.
- W. M. Bowyer. *Greenwich Observations*, 1908.
- W. M. Bowyer. *Greenwich Observations*, 1909.
- W. M. Bowyer. *Greenwich Catalog of Double Stars*, 1921.
- S. J. Brown. *Publications of the U.S. Naval Observatory Second Series*, 6:A117, 1911.
- W. W. Bryant. *Greenwich Observations*, 1900.
- W. W. Bryant. *Greenwich Observations*, 1901a.
- W. W. Bryant. *Greenwich Observations*, 1901b.
- W. W. Bryant. *Greenwich Observations*, 1901c.
- W. W. Bryant. *Greenwich Observations*, 1901d.
- W. W. Bryant. *Greenwich Observations*, 1901e.
- W. W. Bryant. *Greenwich Observations*, 1901f.
- W. W. Bryant. *Greenwich Observations*, 1901g.

- W. W. Bryant. *Greenwich Observations*, F1, 1920.
- W. W. Bryant. *Greenwich Catalog of Double Stars*, 1921.
- S. W. Burnham. the discovery of κ Pegasi as a close double star. *MNRAS*, 41:33–+, November 1880.
- S. W. Burnham. Double-Star Observations. *Astronomische Nachrichten*, 120:289–+, 1889.
- S. W. Burnham. Double Star Observations. *Astronomische Nachrichten*, 124:49–+, 1890.
- S. W. Burnham. Double Star Observations. *Astronomische Nachrichten*, 127:369–+, 1891.
- S. W. Burnham. Double star discoveries and measures. *Astronomische Nachrichten*, 130:257–+, 1892.
- S. W. Burnham. Double Star Observations made at the Lick Observatory in 1892. *Astronomische Nachrichten*, 131:329–+, 1893.
- S. W. Burnham. cited by Lewis. *Memoirs of the Royal Astronomical Society*, 56:1, 1906.
- W. W. Campbell and W. H. Wright. A list of nine stars whose velocities in the line of sight are variable. *ApJ*, 12:254–257, November 1900.
- M. P. Candy. *R. Obs. Bul.*, 88, 1964.
- M. P. Candy. *R. Obs. Bul.*, 184, 1979.
- M. M. Colavita, J. K. Wallace, B. E. Hines, Y. Gursel, F. Malbet, D. L. Palmer, X. P. Pan, M. Shao, J. W. Yu, A. F. Boden, P. J. Dumont, J. Gubler, C. D. Koresko, S. R. Kulkarni, B. F. Lane, D. W. Mobley, and G. T. van Belle. The Palomar Testbed Interferometer. *ApJ*, 510:505–521, January 1999.
- G. C. Comstock. Observations of double stars. *Publications of the Washburn Observatory*, 10, 1896.
- G. C. Comstock. *Publications of the Washburn Observatory*, 10 Part 3, 1906.
- G. C. Comstock. Observations of double stars, 1907-1919. *Publications of the Washburn Observatory*, 10:2–+, 1921.
- P. Couteau. Mesures d'étoiles doubles faites aux Observatoires Yerkes et McDonald. *Journal des Observateurs*, 45:225–+, 1962.

- P. Couteau. Mesures d'étoiles doubles faites au réfracteur de 38 cm de l'Observatoire de Nice. *Journal des Observateurs*, 46:155–+, 1963.
- P. Couteau. Mesures d'étoiles doubles faites au réfracteur de 38 cm de l'Observatoire de Nice. *Journal des Observateurs*, 49:341–+, 1966.
- P. Couteau. Mesures d'étoiles doubles faites à Nice aux lunettes de 50 et de 74 CM. *A&AS*, 3:51–+, November 1970.
- P. Couteau. Mesures d'étoiles doubles faites à Nice. *A&AS*, 6:185–+, June 1972.
- P. Couteau. Measurements of double stars made at Nice. *A&AS*, 20:391–+, June 1975.
- P. Couteau. Measurements of double stars at Nice with 74-cm and 50-cm refractors. *A&AS*, 60:241–259, May 1985.
- P. Couteau. Measurements of binary stars obtained at Pic-du-Midi and at Nice. *A&AS*, 79:385–389, September 1989.
- P. Couteau and J. Ling. Binary star measurements made at Pic-du-Midi. *A&AS*, 73:449–451, June 1988.
- E. Doolittle. Measures of 1066 double and multiple stars made with the eighteen-inch refractor of the Flower Astronomical Observatory. *Publications of the Flower and Cook Astronomical Observatory*, 2:1–+, 1905.
- E. Doolittle. Stars, Double and multiple, Measures of double stars. *MNRAS*, 75:666–+, June 1915.
- F. Dyson. *Greenwich Observations*, 1895.
- R. Engelmann. Doppelsternmessungen. *Astronomische Nachrichten*, 112:193–+, 1885.
- W. S. Finsen. *Union Obs. Circ.*, 6:170, 1953.
- W. S. Finsen. *Union Obs. Circ.*, 6:259, 1956.
- P. Fox. Measures of Double Stars. *Annales of the Dearborn Observatory*, 2:1–219, 1925.
- H. Fu, W. I. Hartkopf, B. D. Mason, H. A. McAlister, E. G. Dombrowski, T. Westin, and O. G. Franz. ICCD Speckle Observations of Binary Stars. XVI. Measurements During 1982-1989 from the Perkins 1.8-M Telescope. *AJ*, 114:1623–+, October 1997.
- H. Furner. *Greenwich Observations*, 1905.

- H. Furner. *Greenwich Observations*, 1906.
- H. Furner. *Greenwich Observations*, B1, 1927.
- H. Furner. *Greenwich Observations*, B1, 1935.
- R. Gili. Measures of Double Stars Made at the Great Refractor of Nice - Part One. *Astronomische Nachrichten*, 312:41–+, 1991.
- R. Gili and D. Bonneau. CCD measurements of visual double stars made with the 74 cm and 50 cm refractors of the Nice Observatory (2nd series). *A&A*, 378:954–957, November 2001.
- W. I. Hartkopf, B. D. Mason, H. A. McAlister, L. C. Roberts, N. H. Turner, T. A. ten Brummelaar, C. M. Prieto, J. F. Ling, and O. G. Franz. ICCD Speckle Observations of Binary Stars. XXIII. Measurements during 1982-1997 from Six Telescopes, with 14 New Orbits. *AJ*, 119:3084–3111, June 2000.
- W. I. Hartkopf, B. D. Mason, G. L. Wycoff, and H. A. McAlister. Fourth catalog of interferometric measurements of binary stars. <http://ad.usno.navy.mil/wds/int4.html>, 2004.
- W. I. Hartkopf, H. A. McAlister, and O. G. Franz. Binary star orbits from speckle interferometry. II - Combined visual-speckle orbits of 28 close systems. *AJ*, 98:1014–1039, September 1989.
- W. I. Hartkopf, H. A. McAlister, and O. G. Franz. ICCD speckle observations of binary stars. VI - Measurements during 1989-1990 from the Kitt Peak 4 M telescope. *AJ*, 104:810–820, August 1992.
- W. I. Hartkopf, H. A. McAlister, B. D. Mason, D. J. Barry, N. H. Turner, and H. Fu. ICCD speckle observations of binary stars. 11: Measurements during 1991-1993 from the Kitt Peak 4 M telescope. *AJ*, 108:2299–2311, December 1994.
- W. I. Hartkopf, H. A. McAlister, B. D. Mason, T. T. Brummelaar, L. C. Roberts, N. H. Turner, and J. W. Wilson. ICCD Speckle Observations of Binary Stars. XVII. Measurements During 1993-1995 From the Mount Wilson 2.5-M Telescope. *AJ*, 114: 1639–+, October 1997.
- W. D. Heintz. Mikromettermessungen von Doppelsternen IV. *Journal des Observateurs*, 46: 1–+, 1963.

- W. D. Heintz. Micrometer observations of double stars and new pairs. XI. *ApJS*, 51:249–268, February 1983.
- F. Henroteau. Buletin Number 304 - A prectrographic study of kappa Pegasi. *Lick Observatory Bulletin*, 9:120–127, 1918.
- F. Holden. Measures of double stars. *Journal des Observateurs*, 46:133–+, 1963.
- F. Holden. Double Star Measures at Lick Observatory, Mount Hamilton, California. *PASP*, 86:902–+, December 1974.
- F. Holden. Micrometric measures of visual double stars. *PASP*, 87:253–257, April 1975.
- F. Holden. Double star measures at Lick Observatory Mount Hamilton California. *PASP*, 88:325–333, June 1976.
- F. Holden. Double star measures at Lick Observatory, Mount Hamilton, California. *PASP*, 90:465–472, August 1978.
- E. Horch, Z. Ninkov, W. F. van Altena, R. D. Meyer, T. M. Girard, and J. G. Timothy. Speckle Observations of Binary Stars with the WIYN Telescope. I. Measures During 1997. *AJ*, 117:548–561, January 1999.
- K. A. Innanen, J. Q. Zheng, S. Mikkola, and M. J. Valtonen. The Kozai Mechanism and the Stability of Planetary Orbits in Binary Star Systems. *AJ*, 113:1915–+, May 1997.
- R. M. Ismailov. Interferometric observations of double stars in 1986-1990. *A&AS*, 96:375–377, December 1992.
- S. Isobe, Y. Norimoto, M. Noguchi, J. Ohtsubo, and N. Baba. Speckle observations of visual and spectroscopic binaries. *Publications of the National Astronomical Observatory of Japan*, 1:217–225, 1990a.
- S. Isobe, Y. Norimoto, M. Noguchi, J. Ohtsubo, and N. Baba. Speckle observations of visual and spectroscopic binaries. II. *Publications of the National Astronomical Observatory of Japan*, 1:381–392, 1990b.
- H. M. Jeffers. *Unpublished*.
- H. M. Jeffers. Bulletin Number 518 - Measures of double stars. *Lick Observatory Bulletin*, 19:175–181, 1939.

- G. H. Kaplan, J. A. Hughes, P. K. Seidelmann, C. A. Smith, and B. D. Yallop. Mean and apparent place computations in the new IAU system. III - Apparent, topocentric, and astrometric places of planets and stars. *AJ*, 97:1197–1210, April 1989.
- L. G. Kiseleva, P. P. Eggleton, and S. Mikkola. Tidal friction in triple stars. *MNRAS*, 300:292–302, October 1998.
- M. Konacki. Precision Radial Velocities of Double-lined Spectroscopic Binaries with an Iodine Absorption Cell. *ApJ*, 626:431–438, June 2005.
- Y. Kozai. Secular perturbations of asteroids with high inclination and eccentricity. *AJ*, 67:591–+, November 1962.
- G. P. Kuiper. Visual measures of double stars made in the years 1929.6–1931.3. *Bull. Astron. Inst. Netherlands*, 7:129–+, December 1933.
- B. F. Lane and M. W. Muterspaugh. Differential Astrometry of Subarcsecond Scale Binaries at the Palomar Testbed Interferometer. *ApJ*, 601:1129–1135, February 2004.
- J. Le Beau. *Obs. Trav. Soc. Astron. France*, 9:41, 1987.
- J. Le Beau. Binary star measurements made at Nice with the 50-cm reflector. *A&AS*, 77:125–130, January 1989.
- F. P. Leavenworth. Double-star observations. *AJ*, 16:195–196, August 1896.
- F. P. Leavenworth. Micrometrical measures of double stars. *AJ*, 29:17–24, March 1915.
- F. P. Leavenworth. Micrometric measures of double stars. *AJ*, 30:115–122, March 1917.
- F. P. Leavenworth. Micrometric measures of double stars. *AJ*, 32:129–133, December 1919.
- T. Lewis. Note on the orbit of κ Pegasi (β 989). *MNRAS*, 55:17–+, November 1894.
- T. Lewis. *Greenwich Observations*, 1895.
- T. Lewis. *Greenwich Observations*, 1896.
- T. Lewis. *Greenwich Observations*, 1897.
- T. Lewis. *Greenwich Observations*, 1898.
- T. Lewis. *Greenwich Observations*, 1899.
- T. Lewis. *Greenwich Observations*, 1900.

- T. Lewis. *Greenwich Observations*, 1901.
- T. Lewis. *Greenwich Observations*, 1902.
- T. Lewis. *Greenwich Observations*, 1903.
- T. Lewis. *Greenwich Observations*, 1904.
- T. Lewis. *Greenwich Observations*, 1905.
- T. Lewis. *Greenwich Observations*, 1906.
- T. Lewis. *Greenwich Observations*, 1907.
- T. Lewis. *Greenwich Observations*, 1908.
- T. Lewis. *Greenwich Observations*, 1909.
- T. Lewis. *Greenwich Catalog of Double Stars*, 1921.
- J. Ling and P. Couteau. Measurements of binary stars made at PIC DU Midi and Nice. *A&AS*, 95:423–427, November 1992.
- J. F. Ling and C. Prieto. Micrometer measurements of visual double stars made at the Cote d’Azur Observatory. *Astronomische Nachrichten*, 318:365–367, November 1997.
- W. J. Luyten. The Triple System of κ Pegasi. *ApJ*, 79:449–+, June 1934.
- M. Maggini. *Publications of Osservatorio Astrofisico di Catania*, 1925.
- W. Markowitz. Observations of double stars, 1949-52 : and a study of the optics of the 26-inch refractor. *Publications of the U.S. Naval Observatory Second Series*, 17:194–269, 1956.
- C. Martin, F. Mignard, W. I. Hartkopf, and H. A. McAlister. Mass determination of astrometric binaries with Hipparcos. III. New results for 28 systems. *A&AS*, 133:149–162, December 1998.
- B. D. Mason, W. I. Hartkopf, E. R. Holdenried, and T. J. Rafferty. Speckle Interferometry of New and Problem Hipparcos Binaries. II. Observations Obtained in 1998-1999 from McDonald Observatory. *AJ*, 121:3224–3234, June 2001a.
- B. D. Mason, C. Martin, W. I. Hartkopf, D. J. Barry, M. E. Germain, G. G. Douglass, C. E. Worley, G. L. Wycoff, T. Ten Brummelaar, and O. G. Franz. Speckle Interferometry of New and Problem HIPPARCOS Binaries. *AJ*, 117:1890–1904, April 1999.

- B. D. Mason, G. L. Wycoff, W. I. Hartkopf, G. G. Douglass, and C. E. Worley. The 2001 US Naval Observatory Double Star CD-ROM. I. The Washington Double Star Catalog. *AJ*, 122:3466–3471, December 2001b.
- M. Mayor and T. Mazeh. The frequency of triple and multiple stellar systems. *A&A*, 171: 157–177, January 1987.
- H. McAlister, W. I. Hartkopf, and O. G. Franz. ICCD speckle observations of binary stars. V - Measurements during 1988-1989 from the Kitt Peak and the Cerro Tololo 4 M telescopes. *AJ*, 99:965–978, March 1990.
- H. A. McAlister. Speckle interferometric measurements of binary stars. I. *ApJ*, 215:159–165, July 1977.
- H. A. McAlister. Speckle interferometric measurements of binary stars. II. *ApJ*, 225:932–938, November 1978.
- H. A. McAlister. Speckle interferometric measurements of binary stars. IV. *ApJ*, 230:497–501, June 1979.
- H. A. McAlister and F. C. Fekel. Speckle interferometric measurements of binary stars. V. *ApJS*, 43:327–337, June 1980.
- H. A. McAlister and W. I. Hartkopf. Catalog of Interferometric Measurements of Binary Stars, CHARA Contribution No. 1. 1984.
- H. A. McAlister, W. I. Hartkopf, E. M. Hendry, B. G. Campbell, and F. C. Fekel. Speckle interferometric measurements of binary stars. VIII. *ApJS*, 51:309–320, March 1983.
- H. A. McAlister, W. I. Hartkopf, J. R. Sowell, E. G. Dombrowski, and O. G. Franz. ICCD speckle observations of binary stars. IV - Measurements during 1986-1988 from the Kitt Peak 4 M telescope. *AJ*, 97:510–531, February 1989.
- H. A. McAlister and E. M. Hendry. Speckle interferometric measurements of binary stars. VI. *ApJS*, 48:273–278, March 1982a.
- H. A. McAlister and E. M. Hendry. Speckle interferometric measurements of binary stars. VII. *ApJS*, 49:267–272, June 1982b.
- E. Merlin. Observations d'étoiles doubles effectuées à l'équatorial de 38 centime très EN 1906 et 1907. *Annales de l'Observatoire royal de Belgique. Annales astronomiques ; nouv. ser., t. 11, Bruxelles : Hayez, 1908., p. [75]-95 ; 32 cm., 11:75–+, 1908.*

- N. Miura, N. Baba, M. Ni-Ino, J. Ohtsubo, M. Noguchi, and S. Isobe. Speckle observations of visual and spectroscopic binaries. IV. *Publications of the National Astronomical Observatory of Japan*, 2:561–571, 1992.
- N. Miura, M. Ni-Ino, N. Baba, T. Iribe, and S. Isobe. Speckle observations of visual and spectroscopic binaries. V. *Publications of the National Astronomical Observatory of Japan*, 3:153–167, 1993.
- P. J. Morel. Mesures d'étoiles doubles visuelles. *A&AS*, 3:71–+, November 1970.
- P. J. Morel. Visual Double Stars Measurements. *A&AS*, 46:3–+, October 1981.
- P. Muller. Mesures d'Etoiles Doubles faites à Strasbourg en 1948-50. *Journal des Observateurs*, 33:105–+, January 1950.
- P. Muller. Mesures d'Etoiles Doubles effectuées à l'Observatoire du Pic-du-Midi en juillet-août 1951. *Journal des Observateurs*, 34:81–+, January 1951.
- P. Muller. Double star observations at Lick Observatory. *AJ*, 59:388–+, November 1954a.
- P. Muller. Mesures d'étoiles doubles faites à Strasbourg en 1952-1953. *Journal des Observateurs*, 37:125–+, January 1954b.
- P. Muller. Mesures d'étoiles doubles faites à Strasbourg en 1954. *Journal des Observateurs*, 38:221–+, January 1955.
- P. Muller. Observations d'étoiles doubles faites au Pic-du-Midi en septembre octobre 1957. *Journal des Observateurs*, 41:109–+, January 1958.
- P. Muller. Mesures d'étoiles doubles a Meudon (3eme et derniere serie). *A&AS*, 23:205–221, January 1976.
- M. W. Muterspaugh, B. F. Lane, M. Konacki, B. F. Burke, M. M. Colavita, S. R. Kulkarni, and M. Shao. Phases differential astrometry and the mutual inclination of the v819 herculis triple star system. Submitted for publication in *Å.*, 2005.
- M. A. C. Perryman, L. Lindegren, J. Kovalevsky, E. Hoeg, U. Bastian, P. L. Bernacca, M. Crézé, F. Donati, M. Grenon, F. van Leeuwen, H. van der Marel, F. Mignard, C. A. Murray, R. S. Le Poole, H. Schrijver, C. Turon, F. Arenou, M. Froeschlé, and C. S. Petersen. The HIPPARCOS Catalogue. *A&A*, 323:L49–L52, July 1997.
- W. Rabe. Beobachtungen von Doppelsternen 1913 bis 1916. *Astronomische Nachrichten*, 217:413–+, January 1923.

- W. Rabe. Mikrometermessungen von Doppelsternen. *Veroeffentlichungen der Sternwarte Munchen*, 1, 1939.
- W. Rabe. *Mikrometermessungen von Doppelsternen in den Jahren 1932 bis 1946*. Berlin, Akademie-Verlag, 1953., 1953.
- W. Rabe and W. D. Heintz. Doppelsternbahnen. *Veroeffentlichungen der Sternwarte Munchen*, 6:113–123, 1961.
- G. V. Schiaparelli. *Osservazioni sulle stelle doppie. Serie seconda: comprendente le misure DI 636 sistemi eseguite col refrattore equatoriale Merz-Repsold negli anni 1886-1900*. Milano, U. Hoepli, 1909., 1909.
- G. D. Schmidt, J. R. P. Angel, and R. Harms. Speckle interferometry with a linear digicon detector. *PASP*, 89:410–414, June 1977.
- T. J. J. See. *Publications of the U.S. Naval Observatory Second Series*, 6:A117, 1911.
- G. V. Simonov. Visual measures of double stars 6th series, 1936-1940 /. *Annals of the Bosscha Observatory Lembang (Java) Indonesia*, 9, 1951.
- S. Söderhjelm. Visual binary orbits and masses post hipparcos. *A&A*, 341:121–140, 1999.
- G. Struve. *Publ. Berlin Babelsberg Obs.*, 14 Pt. 1, 1962.
- H. Struve. *Pulkova Publ. Ser. 2*, 12, 1901.
- L. S. T. Symms. *R. Obs. Bull.*, 88, 1964.
- A. A. Tokovinin. Interferometric Observations of Double Stars. *Astronomicheskij Tsirkulyar*, 1097:3–+, 1980.
- A. A. Tokovinin. Interferometer observations of double stars. I. *Soviet Astronomy Letters*, 8:22–24, February 1982a.
- A. A. Tokovinin. Interferometer observations of double stars. II. *Soviet Astronomy Letters*, 8:99–101, April 1982b.
- A. A. Tokovinin. Interferometer Observations of Double Stars - Part Three. *Soviet Astronomy Letters*, 9:293–+, June 1983.
- A. A. Tokovinin. Interferometric observations of double stars in 1983 and 1984. *A&AS*, 61: 483–486, September 1985.

- A. A. Tokovinin and R. M. Ismailov. Interferometric Observations of Double Stars in 1985 and 1986. *A&AS*, 72:563–+, March 1988.
- G. van Biesbroeck. Observations d'étoiles doubles et discussion des mesures. *Annales de l'Observatoire Royal de Belgique Nouvelle serie*, 9:1–144, 1904.
- G. van Biesbroeck. Measurements of double stars. *Publications of the Yerkes Observatory*, 5:1–+, 1927.
- G. van Biesbroeck. *Publications of the Yerkes Observatory*, 8:47, 1936.
- G. van Biesbroeck. *Publications of the Yerkes Observatory*, 8 pt. 6, 1954.
- G. van Biesbroeck. *Publications of the Yerkes Observatory*, 9 pt. 2, 1960.
- G. van Biesbroeck. Micrometric Measures of Double Stars. *ApJS*, 28:413–+, November 1974.
- P. van de Kamp. A determination of the parallax and mass-ratio Of K Pegasi. *AJ*, 53:34–+, October 1947.
- W. H. van den Bos. *Ann. Leiden Obs.*, 14 pt. 3, 1925.
- W. H. van den Bos. *Publications of the Yerkes Observatory*, 9 pt. 1, 1960.
- W. H. van den Bos. Micrometer measures of double stars. *AJ*, 67:141–+, March 1962a.
- W. H. van den Bos. Micrometer Measures of Double Stars. II. *AJ*, 67:555–+, October 1962b.
- W. H. van den Bos. Micrometer measures of doubles stars. III. *AJ*, 68:57–+, February 1963.
- F. van Leeuwen, D. W. Evans, M. Grenon, V. Grossmann, F. Mignard, and M. A. C. Perryman. The HIPPARCOS mission: photometric data. *A&A*, 323:L61–L64, July 1997.
- J. Voûte. Observations of double stars. *Ricerche Astronomiche*, 2:319–+, 1951.
- J. Voûte. Mesures of double stars, war-seris, made at the Bosscha Observatory Lembang (Java). *Journal des Observateurs*, 38:109–+, January 1955.
- J. G. Voûte. *Annals of the Bosscha Observatory Lembang (Java) Indonesia*, 6 pt. 4:D1, 1947.
- R. L. Walker. Micrometer measures of 711 double stars. *Publications of the U.S. Naval Observatory Second Series*, 25:1–+, 1985.
- R. H. Wilson. *Publ. Univ. Penn.*, 6.4:3, 1941a.

- R. H. Wilson. *Publ. Univ. Penn.*, 6.4:21, 1941b.
- R. H. Wilson. Observations of double stars. *AJ*, 55:153–+, August 1950.
- R. H. Wilson. Observations of double stars - Summer 1950. *AJ*, 56:69–+, May 1951.
- R. H. Wilson. Double star observations in 1951. *AJ*, 57:248–+, December 1952.
- R. H. Wilson. Double stars observations in 1953. *AJ*, 59:256–+, August 1954a.
- R. H. Wilson. Observations of double stars in 1952. *AJ*, 59:132–+, April 1954b.
- R. H. Wilson. Double star observations in 1954. *AJ*, 60:446–+, December 1955.
- R. H. Wilson. Visual measures of 193 double and multiple stars. *A&AS*, 35:193–195, February 1979.
- C. E. Worley. Measures of 278 double stars. *AJ*, 67:403–+, August 1962.
- C. E. Worley. Micrometer measures of 1164 double stars. *Publications of the U.S. Naval Observatory Second Series*, 18:1–+, 1967.
- C. E. Worley. Micrometer measures of 401 double stars. *AJ*, 77:878–+, December 1972.
- C. E. Worley. Micrometer measures of 1,980 double stars. *Publications of the U.S. Naval Observatory Second Series*, 24:1–+, 1978.
- J.-P. Zahn. Tidal friction in close binary stars. *A&A*, 57:383–394, May 1977.